The running of the electromagnetic coupling α in small angle Bhabha scattering

A.B. Arbuzov[1], D. Haidt[2], C. Matteuzzi[3], M. Paganoni[3], L. Trentadue[4,a]

[1] BLTP, Joint Institute for Nuclear Research, Dubna, 141980, Russia
[2] DESY, Notkestr. 85, 22603 Hamburg, Germany
[3] Dipartimento di Fisica, Università di Milano-Bicocca and INFN-Milano, Piazza della Scienza 3, 20126 Milan, Italy
[4] CERN Theory Division, 1211 Geneva 23, Switzerland

Abstract. A method to determine the running of α from a measurement of small angle Bhabha scattering is proposed and worked out. The method is suited to high statistics experiments at e^+e^--colliders which are equipped with luminometers in the appropriate angular region. A new simulation code predicting small angle Bhabha scattering is also presented.

1 Introduction

The electroweak standard model $SU(2) \otimes U(1)$ contains as a constitutive part quantum electrodynamics (QED). The running of the electromagnetic coupling α is determined by the theory:

$$\alpha(q^2) = \frac{\alpha(0)}{1 - \Delta\alpha(q^2)}, \tag{1}$$

where $\alpha(0) = \alpha_0$ is the Sommerfeld fine structure constant, which has been measured to a precision of $3.7 \cdot 10^{-9}$ [1]. A positive $\Delta\alpha(q^2)$ arises from loop contributions to the photon propagator. The numerical prediction of electroweak observables involves the knowledge of $\alpha(q^2)$, usually for $q^2 \neq 0$. For instance, the knowledge of $\alpha(m_Z^2)$ is relevant for the evaluation of quantities measured by the LEP experiments. This is achieved by evolving α from $q^2 = 0$ up to the Z mass scale $q^2 = m_Z^2$. The evolution expressed by the quantity $\Delta\alpha$ receives contributions from leptons, hadrons and the gauge bosons. The hadronic contribution to the vacuum polarisation, which cannot be calculated from first principles, is estimated with the help of a dispersion integral and evaluated [2] by using total cross section measurements of $e^+e^- \rightarrow$ hadrons at low energies. Therefore, any evolved value $\alpha(q^2)$, particularly for $|q^2| > 4m_\pi^2$, is affected by uncertainties originating from hadronic contributions. The uncertainty on $\alpha(m_Z^2)^{-1}$ induced by these data is as small as ± 0.09 [2]; nevertheless it turned out [3] that it limits the accurate prediction of electroweak quantities within the standard model, particularly for the prediction of the Higgs mass.
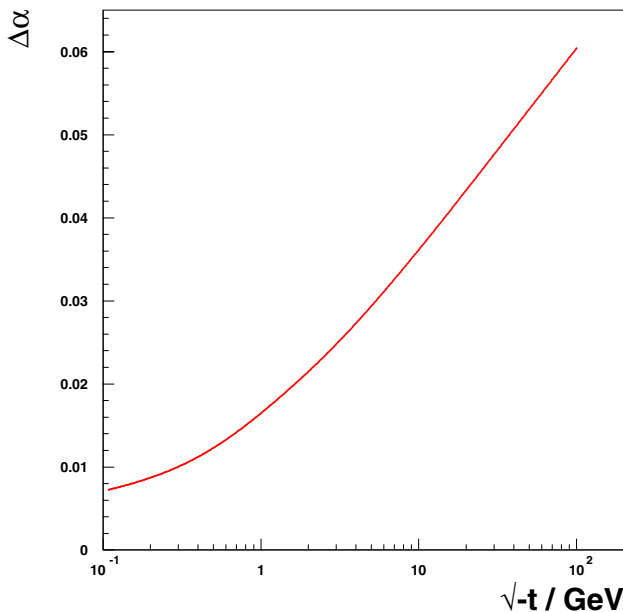
While waiting for improved measurements from BEPC, VEPP-4M and DAFNE as input to the dispersion integral, intense efforts are made to improve on estimating the hadronic shift $\Delta\alpha_{\text{had}}$, as for instance in [4–7], and to find alternative ways of measuring α itself. Attempts have been made to measure $\alpha(q^2)$ directly using e^+e^--data at various energies, such as measuring the ratio of $e^+e^-\gamma/e^+e^-$ [8] or more directly the angular distribution of Bhabha scattering [9].

In this article the running of α is studied using small angle Bhabha scattering. This process provides unique information on the QED coupling constant α at low *spacelike* momentum transfer $t = -|q^2|$, where

$$t = -\frac{1}{2} \, s \, (1 - \cos\theta) \tag{2}$$

is related to the total invariant energy $\sqrt{s}$ and the scattering angle θ of the final state electron. The small angle region has the virtue of giving access to values of $\alpha(t)$ without being affected by weak contributions. The cross section can be theoretically calculated with a precision at the per mille level. It is dominated by the photonic t-channel exchange, and the non-QED contributions have been computed [10] and are on the order of 10^{-4} (see Table 1); in particular contributions from boxes with two weak bosons are safely negligible.

In general, the Bhabha cross section is computed (see Sect. 3) from the entire set of gauge invariant amplitudes in both the s- and the t-channel. Consequently, two invariant scales s and t govern the process. The different amplitudes are functions of both s and t and also the QED coupling α appears as $\alpha(s)$ respectively $\alpha(t)$ [11]. However, the restriction of Bhabha scattering to the kinematic regime of small angles results in a considerable simplifi-

---

[a] *Permanent address*: Dipartimento di Fisica, Università di Parma and INFN, Gruppo Collegato di Parma, 43100 Parma, Italy

Fig. 1. $\Delta\alpha$ versus $\sqrt{-t}$ in units of GeV in the spacelike region

Fig. 2. Contributions to $\Delta\alpha$ from leptons (dashed curve) and hadrons (solid curve) versus $\sqrt{-t}$ in units of GeV

cation, since then the s-channel contribution gives only a negligible contribution, as is quantitatively demonstrated in Table 1. Thus, the measurement of the angular distribution allows one indeed to verify directly the running of the coupling $\alpha(t)$. For the actual calculations $\theta \gg m_e/E_{\mathrm{beam}}$ and $E_{\mathrm{beam}} \gg m_e$ must be satisfied (see Sect. 4.1). Obviously, in order to manifest the running, the experimental precision must be adequate.

This idea can be realized by high statistics experiments at e^+e^--colliders equipped with finely segmented luminometers, in particular by the LEP experiments given their large event samples, by SLC, and future Linear Colliders. The relevant luminometers cover the t-range from a few GeV^2 to order $100\,\mathrm{GeV}^2$.

The t-dependence of the quantity $\Delta\alpha(t)$, (1) and (2), at small values of t is illustrated in Fig. 1.

It shows the predicted running of α in the relevant spacelike region. The figure is obtained using the program alphaQED by Jegerlehner [2]. At low energies (see Fig. 2) $\Delta\alpha$ is dominated by the contribution from the leptons, while with increasing energy also the contribution involving hadrons gets relevant. The region where hadronic corrections are critical is contained in the considered t-range.

2 The method

The experimental determination of the angular distribution of the Bhabha cross section requires the precise definition of a Bhabha event in the detector. The analysis follows closely the procedure adopted in the luminosity measurement which is described in detail, for instance, in [12], and elaborates on the additional aspect related to the measurement of a differential quantity. To this aim the luminosity detector must have a sufficiently large angular acceptance and adequate fine segmentation. The variable t, see (2), is reconstructed on an event-by-event basis.
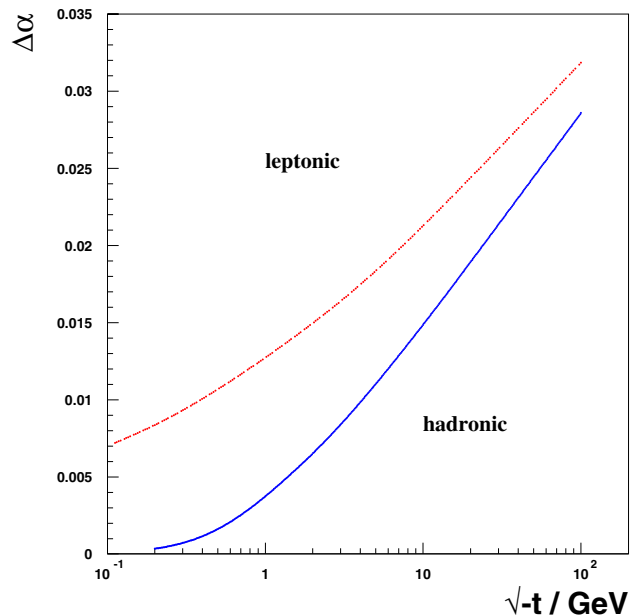
The method to measure the running of α exploits the fact that the cross section for the process $e^+e^- \to e^+e^-$ can be conveniently decomposed into three factors:

$$\frac{\mathrm{d}\sigma}{\mathrm{d}t} = \frac{\mathrm{d}\sigma^0}{\mathrm{d}t} \left(\frac{\alpha(t)}{\alpha(0)} \right)^2 (1 + \Delta r(t)) \tag{3}$$

as worked out in Sect. 3. All three factors are predicted to a precision of 0.1% or better. The first factor on the right hand side refers to the effective Bhabha Born cross section including soft and virtual photons according to [10], which is precisely known, and which accounts for the strongest dependence on t. The vacuum polarization effect in the leading photon t-channel exchange is incorporated in the running of α and gives rise to the squared factor in (3). The third factor $\Delta r(t)$ collects all the remaining real (in particular collinear) and virtual radiative effects not incorporated in the running of α. The experimental data after correction for detector effects is to be compared with (3). The t-dependence is rather steep; thus migration effects may need attention.

This goal is achieved by using a newly developed program based on the already existing semi-analytical code NLLBHA [10,13]. A detailed description of this code, called SAMBHA, is given in Sect. 4.

3 Theory

It is convenient to confront the fully corrected measured cross section with the Bhabha cross section including radiative corrections in the factorized form given by (3). The physical cross section is infrared safe [10]. This decomposition is neither unique nor dictated by a compelling physical reason, rather it allows one to separate the different sources

of t-dependence in a transparent way without introducing any additional theoretical uncertainty. The various factors are discussed one by one in the following subsections.

3.1 The cross section $\mathrm{d}\sigma^0/\mathrm{d}t$

The differential cross section $\mathrm{d}\sigma^0/\mathrm{d}t$ is defined by

$$\frac{\mathrm{d}\sigma^0}{\mathrm{d}t} = \frac{\mathrm{d}\sigma^B}{\mathrm{d}t}\left(\frac{\alpha(0)}{\alpha(t)}\right)^2 . \tag{4}$$

The factor $\mathrm{d}\sigma^B/\mathrm{d}t$ is the Bhabha cross section in *improved Born approximation*, which, by definition, includes the running of α. As seen explicitly in the formulae below (see (5)) the factor $\alpha(t)/\alpha(0)$ is not factorized completely in the improved Born cross section. In order to have the factorized form of (3) nevertheless the t-channel contribution to the running of α has been taken out. In this way, $\mathrm{d}\sigma^0/\mathrm{d}t$ contains not only the usual Born t-dependence, i.e. $1/t$, but also some weaker t-dependences arising from s-channel amplitudes with vacuum polarization effects taken into account [10], although numerically small as mentioned above.

The improved Born cross section for Bhabha scattering within the electroweak standard model is precisely known [14–16]. The differential cross section $\mathrm{d}\sigma^B/\mathrm{d}t$ differs from $\mathrm{d}\sigma^0/\mathrm{d}t$ by the inclusion of those radiative corrections which affect only the propagator of the exchanged photon. They form a gauge invariant subset of all radiative corrections and are shown explicitly. It is convenient to decompose $\mathrm{d}\sigma^B/\mathrm{d}t$ into the contributions arising from the t-channel (B_t), the s-channel (B_s) and their interference (B_i):

$$\frac{\mathrm{d}\sigma^B}{\mathrm{d}t} = \frac{\pi\alpha_0^2}{2s^2}\mathrm{Re}\left\{B_t + B_s + B_\mathrm{i}\right\}, \tag{5}$$

where

$$B_t = \left(\frac{s}{t}\right)^2\left\{\frac{5+2c+c^2}{(1-\Pi(t))^2} + \xi\frac{2(g_v^2+g_a^2)(5+2c+c^2)}{(1-\Pi(t))}\right.$$
$$\left. + \xi^2\left(4(g_v^2+g_a^2)^2 + (1+c)^2(g_v^4+g_a^4+6g_v^2g_a^2)\right)\right\},$$

$$B_s = \frac{2(1+c^2)}{|1-\Pi(s)|^2}$$
$$+ 2\chi\frac{(1-c)^2(g_v^2-g_a^2) + (1+c)^2(g_v^2+g_a^2)}{1-\Pi(s)}$$
$$+ \chi^2\left[(1-c)^2(g_v^2-g_a^2)^2\right.$$
$$\left. + (1+c)^2(g_v^4+g_a^4+6g_v^2g_a^2)\right],$$

$$B_\mathrm{i} = 2\frac{s}{t}(1+c)^2\left\{\frac{1}{(1-\Pi(t))(1-\Pi(s))}\right.$$
$$+ (g_v^2+g_a^2)\left(\frac{\xi}{1-\Pi(s)} + \frac{\chi}{1-\Pi(t)}\right)$$
$$\left. + (g_v^4+6g_v^2g_a^2+g_a^4)\xi\chi\right\},$$

$$\chi = \frac{s}{s-m_z^2+im_Z\Gamma_Z}\cdot\frac{1}{\sin 2\theta_\mathrm{w}},$$

$$\xi = \frac{t}{t-m_Z^2}\cdot\frac{1}{\sin 2\theta_\mathrm{w}},$$

$$g_a = -\frac{1}{2}, \quad g_v = -\frac{1}{2} + 2\sin^2\theta_\mathrm{w}),$$

$$t = (p_1-q_1)^2 = -\frac{1}{2}\,s\,(1-c),$$

$$c = \cos\theta, \quad \theta = \widehat{\boldsymbol{p}_1\boldsymbol{q}_1}.$$

Here s is the total squared invariant mass, θ_w the electroweak mixing angle and θ the scattering angle between the initial and final electron with momenta $\boldsymbol{p}_1$ and $\boldsymbol{q}_1$ respectively [10].

In Table 1 the cross sections are given in nanobarn for the pure QED and electroweak cases. QED_t denotes the contribution of the t-channel pure QED Feynman diagrams. The cross sections are integrated over two relevant angular ranges. The table shows that the t-channel photon exchange dominates the cross section at small angles and justifies why the process is suited for investigating the t-dependence, and so the running of $\alpha(t)$.

By comparing the values of the electroweak cross section with the pure QED one, it is seen that the Z-boson exchange gives a negligible contribution to small angle scattering. In the last two lines (EW+VP$_t$ and EW+VP) there are numbers for the cross section with vacuum polarization (VP) taken into account in the t-channel only, and in all channels, correspondingly. One can see that the effect of s-channel vacuum polarization is small, as a result of the smallness of the s-channel photon-exchange contribution itself. The last line in the table corresponds to the complete formula in (5).

3.2 The running of α

In (5) the two-point functions $\Pi(t) = \Delta\alpha(t)$ and $\Pi(s) = \Delta\alpha(s)$ are responsible for the running of α in the spacelike and timelike regions. In the language of Feynman diagrams the effect arises from fermion loop insertions into the virtual photon lines. We have

$$\Pi(t) = \frac{\alpha_0}{\pi}\left(\delta_t + \frac{1}{3}L - \frac{5}{9}\right)$$
$$+ \left(\frac{\alpha_0}{\pi}\right)^2\left(\frac{1}{4}\,L + \zeta(3) - \frac{5}{24}\right)$$
$$+ \left(\frac{\alpha_0}{\pi}\right)^3\Pi^{(3)}(t) + \mathcal{O}\left(\frac{m_e^2}{t}\right),$$

where

$$L = \ln\frac{Q^2}{m_e^2}, \quad Q^2 = -t, \quad \zeta(3) = 1.202,$$

and where the leading part of the two-loop contribution to the polarization operator is taken into account. The most significant part arises from the electrons and is $L/3 - 5/9$.

Table 1. Various cross sections in nb as a function of the center-of-mass energy in GeV integrated over the two angular ranges 45–110 mrad and 5–50 mrad. The index t denotes the contribution of the corresponding t-channel Feynman diagrams alone. The last columns are of interest for future Linear Colliders

$\sqrt{s}$ (GeV)	91.187	91.2	189	206	500	1000	3000
			45 mrad $< \theta <$ 110 mrad				
$\sqrt{\langle -t \rangle}$ (GeV)	3.4	3.4	7.1	7.7	18.8	37.5	112.6
QED	51.428	51.413	11.971	10.077	1.7105	0.42763	0.047514
QED$_t$	51.484	51.469	11.984	10.088	1.7124	0.42809	0.047566
EW	51.436	51.413	11.965	10.072	1.7105	0.42871	0.049507
EW+VP$_t$	54.041	54.018	12.743	10.745	1.8590	0.47303	0.055748
EW+VP	54.036	54.013	12.742	10.744	1.8588	0.47296	0.055742
			5 mrad $< \theta <$ 50 mrad				
$\sqrt{\langle -t \rangle}$ (GeV)	1.1	1.1	2.2	2.4	5.8	11.6	34.8
QED	4963.4	4962.0	1155.4	972.54	165.08	41.271	4.5857
QED$_t$	4963.5	4962.1	1155.4	972.57	165.09	41.272	4.5858
EW	4963.4	4962.0	1155.4	972.53	165.08	41.272	4.5885
EW+VP$_t$	5075.0	5073.5	1190.6	1003.3	172.51	43.647	4.9603
EW+VP	5075.0	5073.5	1190.6	1003.3	172.51	43.646	4.9605

The $\mathcal{O}(\alpha)$ and $\mathcal{O}(\alpha^2)$ leptonic vacuum polarization has been known since many years [17]. The third order (three-loop) leptonic contributions $\Pi^{(3)}(t)$ have been recently calculated [18]. In the standard model, δ_t contains contributions from muons, τ-leptons, W-bosons and hadrons:

$$\delta_t = \delta_t^\mu + \delta_t^\tau + \delta_t^W + \delta_t^H ,$$

$$\delta_s = \delta_t \ (t \to s) ,$$

which means that δ_s is obtained from δ_t by substituting s by t [10]. The contributions from the leptons ($l = \mu, \tau$) and from the W are theoretically calculable and given by

$$\delta_t^l = \frac{1}{2}\, v_l \left(1 - \frac{1}{3}v_l^2\right) \ln \frac{v_l + 1}{v_l - 1} + \frac{1}{3}\, v_l^2 - \frac{8}{9} ,$$

$$v_l = \sqrt{1 + \frac{4m_l^2}{Q^2}} ,$$

$$\delta_t^W = \frac{1}{4}\, v_W\, (v_W^2 - 4) \ln \frac{v_W + 1}{v_W - 1} - \frac{1}{2}\, v_W^2 + \frac{11}{6} ,$$

$$v_W = \sqrt{1 + \frac{4M_W^2}{Q^2}} .$$

For $Q^2 \gg m_l^2$ the formula simplifies to

$$\delta_t^l = \frac{1}{3} \ln \frac{Q^2}{m_l^2} - \frac{5}{9} .$$

The hadronic contribution cannot be calculated theoretically; instead, it can be expressed as a dispersion integral involving the experimentally measured e^+e^--cross sections:

$$\delta_t^{\text{had}} = \frac{Q^2}{4\pi\alpha_0^2} \int_{4m_\pi^2}^\infty \frac{\sigma^{e^+e^- \to h}(s')}{s' + Q^2}\, \mathrm{d}s' . \qquad (6)$$

For numerical calculations the hadronic contributions as included in the parametrisation [4,19] are adopted.

This procedure, as usually assumed (see e.g. [5]) is based on the analyticity of the function $\alpha(q^2)$ in the complex plane, except possibly at the energies corresponding to the Landau pole. For the leptonic contributions $\delta_{s,t}^{e,\mu,\tau}$ this assertion is true, while for the hadronic contribution δ_t^{had} it relies on the dispersion approach to the entire, nonperturbative, hadronic physics (see (6)). This ends up in a single analytical function that can be used to deal with the vacuum polarization in the t-channel.

3.3 The radiative factor $1 + \Delta r(t)$ and neglected terms

For the present investigation of the small angle Bhabha cross section consistently only the corrections needed to maintain the required accuracy are kept. All these corrections are included in the new code SAMBHA. All the following contributions have been proven to be negligible [10] and are dropped.

(1) Any electroweak effect beyond the tree level, for instance appearing in boxes or vertices with Z^0- and W-bosons, running weak coupling etc.
(2) Box diagrams at order α^2 and larger.
(3) Contributions of order α^2 without large logarithms, leading from order α^4 (i.e. $\alpha^4 L^4$,...) and subleading higher order ($\alpha^3 L^2$, $\alpha^4 L^3$,...)
(4) Contributions from pair produced hadrons, muons, taus and the corresponding virtual pair corrections to the vertices (estimated to be on the order of $0.5 \cdot 10^{-4}$).

The radiatively corrected Bhabha cross section is denoted by $\mathrm{d}\sigma/\mathrm{d}t$. Numerically it differs from $\mathrm{d}\sigma^B/\mathrm{d}t$ by less than a few percent for small angles depending on energy and final state selection procedure.

4 Monte Carlo codes and comparison

The precise determination of the luminosity at e^+e^--colliders is a crucial ingredient to get an accurate evaluation of all the physically relevant cross sections. They necessarily have to rely on some reference process, which is usually taken to be the small angle Bhabha scattering. Given the high statistical precision provided by the LEP collider, an equally precise knowledge of the theoretical small angle Bhabha cross section is mandatory. In the 1990s the substantial progress in measuring the luminosity reached by the LEP Collaborations has prompted several groups to make a theoretical effort aiming at a 0.1% accuracy [20,21]. This goal has indeed been achieved by developing a dedicated strategy. For the first time small angle Bhabha scattering was evaluated analytically following a new calculation technique [10] yielding the required precision. Analytical calculations have been combined with Monte Carlo programs in order to simulate realistically the conditions of the LEP experiments.

The analytical results evaluated for the various contributions to the observed Bhabha cross section in [10], were implemented into the semi-analytical code NLLBHA (for a short write-up see [13]). The important feature of this code consists in the systematic account of all QED radiative corrections required to reach the *per mille* precision. On the other hand, the simulation of realistic experimental acceptances can only be achieved with Monte Carlo techniques. For this purpose the Monte Carlo code LABSMC was developed [22–24].

4.1 SAMBHA-NLLBHA

The program LABSMC, which was intended to describe large angle Bhabha scattering at high energies, has been complemented with a set of routines from NLLBHA in order to be applicable to small angle Bhabha scattering. This implied the insertion of the relevant second order next-to-leading radiative corrections ($\mathcal{O}(\alpha^2 L)$) in the Monte Carlo code[1] which are crucial to achieve the per mille accuracy. The extension in order to cover small angles resulted in the new code SAMBHA containing the previously existing features together with the following new characteristics:

(1) the complete electroweak matrix element at the Born level;
(2) the complete set of $\mathcal{O}(\alpha)$ QED radiative corrections (including radiation from amplitudes with Z-boson exchange);
(3) vacuum polarization corrections by leptons, hadrons [19], and W-bosons;
(4) one-loop electroweak radiative corrections and effective EW couplings by means of the DIZET v.6.30 [25] package;
(5) higher order leading logarithm photonic corrections by means of the electron structure functions [26–29];

---
[1] The codes are available upon request from the authors.

(6) light pair corrections in the $\mathcal{O}(\alpha^2 L^2)$ leading logarithm approximation including (optionally) the two-photon and singlet mechanisms.

The code is applicable with the following restrictions:

(a) $E_{\text{beam}} \gg m_e$: the energy has to be much larger than the electron mass;
(b) $m_e/E_{\text{beam}} \ll \theta$: extemely small angles are not described well, but the condition is fulfilled in practice both for small and large angle Bhabha measurements in the experiments at LEP, SLC and NLC;
(c) starting from the second order in α, real photon emission is integrated over, i.e. events with two photons separated from electrons are not generated.

4.2 BHLUMI

The Monte Carlo Program BHLUMI, which has been used in the LEP analyses, is decribed in detail in [30].

4.3 Comparison BHLUMI and SAMBHA

BHLUMI is compared with SAMBHA for integral and, for the first time, also differential distributions. The actual measurements are of calorimetric type. Therefore, event samples are generated with both programs subjecting each event to a common set of calorimeter-like criteria (hereafter called CALO).

In a first test the program codes were applied to the conditions established by the working group *Event generators for Bhabha scattering* [12] (YR) with the result that all numbers were reproduced within the quoted accuracy.

In a further test, about 10^8 Bhabha events were generated according to the calorimeter-like conditions specified in Sect. 5.1. This selection rejects a considerable part of events with real hard photon radiation. Therefore, the effect of mutual cancellation between virtual and real radiation is suppressed and inevitably causes fairly large t-dependent radiative corrections. The comparison is made quantitative in the form of the ratio

$$\rho(t) = \frac{\mathrm{d}\sigma_{\text{sambha}}/\mathrm{d}t - \mathrm{d}\sigma_{\text{bhlumi}}/\mathrm{d}t}{\mathrm{d}\sigma_{\text{bhlumi}}/\mathrm{d}t}$$

and displayed in Fig. 3. A linear logarithmic fit to the cross section ratios and their statistical uncertainties gives

$$\rho(t) = -(0.0039 \pm 0.0002)$$
$$-(0.0046 \pm 0.0010) \log \frac{-t}{\langle -t \rangle},$$

with $\langle t \rangle = -8.3 \,\text{GeV}^2$.

The two programs differ significantly in average by 0.4%. At the present level of investigation it cannot be excluded that there is a weak t-dependence.

It is not so surprising to find a discrepancy for the differential quantity, while getting good agreement for the

Table 2. Comparison between the codes NLLBHA(SAMBHA) and BHLUMI. The numbers are obtained using the conditions of Table 19 in [12]. The relative ratio $\delta r/r$ in per mille is defined by (YR-NOW)/YR, The last column gives the relative difference between BHLUMI(NOW) and SAMBHA(NOW)

cut	BHLUMI (YR)	BHLUMI (NOW)	$\delta r/r$	NLLBHA (YR)	NLLBHA (NOW)	$\delta r/r$	
0.1	166.892	166.879	0.07	166.948	166.923	0.14	−0.26
0.3	165.374	165.438	−0.38	165.448	165.420	0.16	0.10
0.5	162.530	162.616	−0.52	162.561	162.25	1.91	2.25
0.7	155.668	155.733	−0.41	155.607	155.40	1.33	2.13
0.9	137.342	137.425	−0.60	137.199	137.32	−0.88	0.76
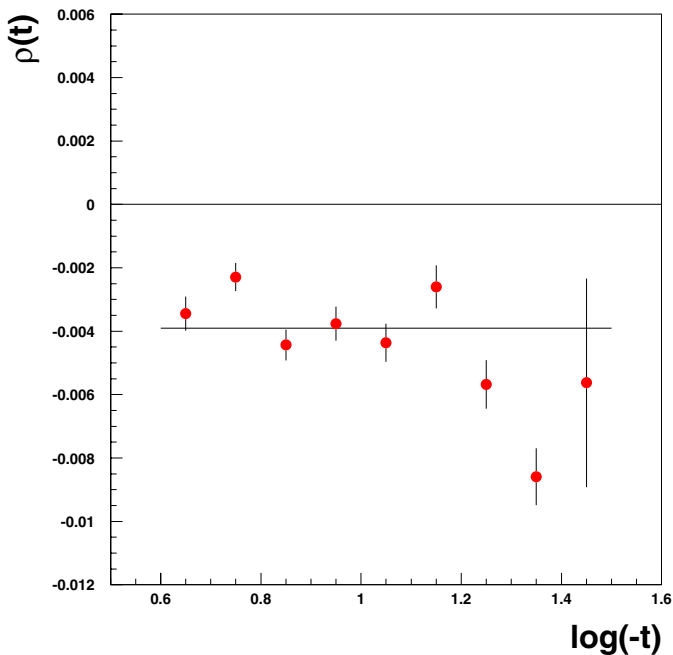
Fig. 3. Cross section ratio $\rho(t)$ versus log $(-t)$ with t in units of GeV^2

integral quantity. In fact, the key element is the far stronger restriction in the event selection for the two cases. In the integral case the events are accepted over the entire angular range of the luminometer, while for the differential analysis the same selection criteria are applied to a set of segments covering eventually the full range of the luminometer. This implies that an event accepted in the integral case, is not necessarily accepted in the differential one due to the more restrictive conditions, such that the sum of events accepted in the segmented luminometer is smaller than the number of events in the full luminometer.

For a quantitative understanding of this qualitative argument a selection of events is presented as a function of the cut $s \cdot x_c = s \cdot x_1 x_2$, where x_i is the fractional energy carried by the electron (or positron) (see Table 2). Obviously, a value for x_c near 1 selects configurations with small acollinearity as opposed to cases with smaller x_c favoring larger acollinearity configurations. For a given opening angle, events with large acollinearity are hardly accepted, in other words the size of the cone opening angle defines the amount of radiative events containing real emitted photons accepted or rejected. Consequently a larger or smaller final

state phase space is probed. Since virtual radiative contributions are unaffected by phase space restrictions, the interplay between real and virtual radiative contributions strongly depends on the acceptance. The accuracy to which radiative corrections have to be treated becomes crucial.

With the tight cuts required for the study of a differential quantity as in the case investigated here, necessarily fine detailed aspects related to radiative contributions are probed. Therefore such studies open a new level of comparison between theory and experiment.

5 Evaluation of the running in a simulated experiment

Anticipating the application of the proposed method to measure the t-dependence of $\alpha(t)$ to the data of a real experiment, a Monte Carlo simulation is carried out instead in order to demonstrate the feasibility. An event sample is generated under the conditions of the DELPHI experiment using the existing program BHLUMI. In the next subsection the sample so obtained is confronted with the expectation of the new program SAMBHA. It should be noted that the t-dependence of $\alpha(t)$, i.e. the quantity to be investigated, is by about an order of magnitude stronger than the possible differences in the intrinsic t-dependences between BHLUMI and SAMBHA (see Sect. 4.3).

5.1 Event generation

The DELPHI detector and its performance is described in [31]. For the analysis the relevant subdetector is the electromagnetic calorimeter STIC [31] covering the extreme forward and backward directions. It has a ring structure with segmentation in both θ and ϕ covering $\sqrt{-t}$-ranges from 1.5 to 6 GeV for LEP1 energies and 3 to 12 GeV for LEP2 energies.

Electrons, positrons and photons are observed as clusters. Their reconstruction is based on a cluster algorithm. The Bhabha events are characterized by two narrow high energy electromagnetic clusters opposite to each other and well inside the detector. The cluster algorithm is applied to the observed energy depositions in the cells of the electromagnetic calorimeter. Furthermore, the cluster with the highest energy satifies the more restrictive requirement to be at the radial position R between 10 and 25 cm such as to cause no inefficiency for the opposite cluster.

Table 3. Table of event numbers generated with BHLUMI. Ring 1 is not considered

$\sqrt{s}$ (GeV)	91.2	189	200
$\int \mathcal{L}\mathrm{d}t$ (pb^{-1})	75	150	200
Ring 2	1844850	863571	1028210
Ring 3	907754	425586	506131
Ring 4	513696	240550	286994
Ring 5	313218	146731	174740
Ring 6	201893	94033	112168

A Monte Carlo simulation has been performed using BHLUMI for three center-of-mass energies of LEP: 91.2 (Z-peak), 189 and 200 GeV. Assuming integrated luminosities $\int \mathcal{L}\mathrm{d}t$ typical for the LEP experiments, the number of events passing the selection criteria are obtained and listed in Table 3. An event is attributed to ring i, if the highest energy cluster is reconstructed in this ring and the criteria listed below are satisfied.

(1) Cluster reconstruction: The main criterion for merging adjacent cells is

$$\left(\frac{\Delta\theta}{30\,\mathrm{mrad}}\right)^2 + \left(\frac{\Delta\phi}{870\,\mathrm{mrad}}\right)^2 < 1\,,$$

where the cluster center is calculated as the energy weighted cell centers.

(2) Only the highest energy cluster in each hemisphere (referred to as F (forward) respectively B (backward)) is considered.

(3) Energy requirements:

$$\min(E_\mathrm{F}, E_\mathrm{B}) > 0.65 E_\mathrm{beam}\,,$$
$$\max(E_\mathrm{F}, E_\mathrm{B}) > 0.94 E_\mathrm{beam}\,.$$

This implies that the Bhabha events have not suffered from sizeable initial state radiation effects.

(4) Geometrical acceptance: The radial position R of the two opposite clusters must satisfy

$$7\,\mathrm{cm} < R_\mathrm{F}, R_\mathrm{B} < 28\,\mathrm{cm}\,.$$

(5) Kinematics: The cluster center and the nominal interaction point of the colliding e^+e^- beams determine the dip angle θ. The quantity t is calculated from the dip angle θ and the nominal center-of-mass energy $\sqrt{s} = 2E_\mathrm{beam}$ according to

$$t = -\tfrac{1}{2}s(1 - \cos\theta_\mathrm{max})\,,$$

where θ_max is defined to be the dip angle of the cluster with the highest energy.

The result of the Monte Carlo experiment is summarized in Table 3. Ring 1 and ring 7 have been disregarded in order to exclude any inefficiency from border effects.

5.2 Comparison and evaluation

In this subsection the relevant observables and the parameters to be extracted are established and discussed.

Each ring defines with its boundaries a bin $(t_\mathrm{min}, t_\mathrm{max})$. The event numbers are to be equated to the corresponding theoretical prediction obtained from the formulae implemented in the program SAMBHA. In order to extract the t-dependence of $\alpha(t)$, (3) is evaluated for each ring R_i defined by the geometry of the DELPHI luminometer. Equation (3) reads then for ring i

$$\sigma_i = \sigma_i^0 \left(\frac{\alpha(t_i)}{\alpha(0)}\right)^2 (1 + \Delta r_i)\,, \tag{7}$$

with the following definitions:

$$\sigma_i = \int^{R_i} \mathrm{d}t \frac{\mathrm{d}\sigma}{\mathrm{d}t}\,,$$

$$\sigma_i^0 = \int^{R_i} \mathrm{d}t \frac{\mathrm{d}\sigma^0}{\mathrm{d}t}\,,$$

$$\left(\frac{\alpha(t_i)}{\alpha(0)}\right)^2 = \int^{R_i} \frac{\mathrm{d}t}{t_\mathrm{max} - t_\mathrm{min}} \left(\frac{\alpha(t)}{\alpha(0)}\right)^2\,,$$

$$1 + \Delta r_i = \left(\frac{\alpha(0)}{\alpha(t_i)}\right)^2 \frac{\sigma_i}{\sigma_i^0}\,.$$

Table 4 contains the resulting theoretical values.

Putting together the experimental and theoretical ingredients, i.e. the observed number of events N_i in each ring together with the relevant luminosities $\int \mathcal{L}\mathrm{d}t$ (from Table 3) and σ_i^0, Δr_i (from Table 4), one obtains the final formula:

$$\left(\frac{\alpha(t_i)}{\alpha(0)}\right)^2 = \frac{N_i}{\sigma_i^0 \int \mathcal{L}\mathrm{d}t} \frac{1}{1 + \Delta r_i}\,, \tag{8}$$

which can be exploited in a linear fit to access the parameters defining the t-dependence of α:

$$\left(\frac{\alpha(t)}{\alpha(0)}\right)^2 = (u_0 \pm \delta u_0) + (u_1 \pm \delta u_1) \cdot \log\frac{-t}{\langle -t \rangle}\,. \tag{9}$$

The parameters of the fit are listed in Table 5.

6 Discussion

Table 5 demonstrates that for the case of the DELPHI setup (see Sect. 5) and assuming typical integrated luminosities, the statistical accuracy is sufficient to verify the running of α for each of the three center-of-mass energies.

Equation (8) can be expanded in terms of $\Delta\alpha$ (see (1)). It is convenient to consider

$$\frac{N_i}{\sigma_i^0} \frac{1}{1 + \Delta r_i} = n_0 + n_1 \log\frac{-t_i}{\langle -t \rangle} \tag{10}$$

rather than (8), since in practice the integrated luminosity $\int \mathcal{L}\mathrm{d}t$ is not known. The two coefficients n_0 and n_1 are

Table 4. Theoretical predictions for each ring of the three factors of (7). For the conditions defined in Sect. 5.1 the angular boundary of ring i is $\theta_i = \arctan(7 + 3(i-1))/220$

No. of ring	1	2	3	4	5	6	7
				$\sqrt{s} = 91.2\,\text{GeV}$			
σ_i^0	63.077	24.728	12.170	6.8694	4.2517	2.8120	1.9552
$(\alpha(t_i)/\alpha(0))^2$	1.0425	1.0475	1.0516	1.0551	1.0582	1.0609	1.0634
$1 + \Delta r_i$	0.9426	0.9440	0.9412	0.9395	0.9240	0.8915	0.7982
				$\sqrt{s} = 189\,\text{GeV}$			
σ_i^0	14.685	5.7563	2.8324	1.5984	0.9889	0.6537	0.4542
$(\alpha(t_i)/\alpha(0))^2$	1.0554	1.0613	1.0661	1.0702	1.0736	1.0767	1.0794
$1 + \Delta r_i$	0.9377	0.9390	0.9360	0.9329	0.9165	0.8858	0.7898
				$\sqrt{s} = 200\,\text{GeV}$			
σ_i^0	13.115	5.1406	2.5295	1.4274	0.8831	0.5838	0.4057
$(\alpha(t_i)/\alpha(0))^2$	1.0565	1.0625	1.0673	1.0714	1.0749	1.0780	1.0807
$1 + \Delta r_i$	0.9376	0.9387	0.9352	0.9330	0.9158	0.8847	0.7896
				$\sqrt{s} = 1000\,\text{GeV}$			
σ_i^0	0.5248	0.2059	0.1014	0.0573	0.0356	0.0236	0.0165
$(\alpha(t_i)/\alpha(0))^2$	1.0921	1.0994	1.1050	1.1096	1.1135	1.1169	1.1199
$1 + \Delta r_i$	0.8622	0.8620	0.8590	0.8545	0.8398	0.8084	0.7205
				$\sqrt{s} = 3000\,\text{GeV}$			
σ_i^0	0.0590	0.0234	0.0117	0.0067	0.0042	0.0028	0.0020
$(\alpha(t_i)/\alpha(0))^2$	1.1192	1.1267	1.1325	1.1373	1.1414	1.1448	1.1479
$1 + \Delta r_i$	0.8467	0.8457	0.8422	0.8381	0.8253	0.7956	0.6975

Table 5. Table of fit results; the uncertainties δu_0 and δu_1 are uncorrelated

$\sqrt{s}$	91.2 GeV	189 GeV	200 GeV
u_0	1.0573 ± 0.0005	1.0698 ± 0.0008	1.0703 ± 0.0007
u_1	0.0242 ± 0.0028	0.0284 ± 0.0041	0.0318 ± 0.0038
$\langle -t \rangle$	$8.5\,\text{GeV}^2$	$36.6\,\text{GeV}^2$	$40.9\,\text{GeV}^2$

obtained from a linear fit and contain the information of both the data and the theory. Their interpretation is

$$n_0 = \int \mathcal{L}\mathrm{d}t \cdot (1 + 2\Delta\alpha(\langle t \rangle)) ,$$

$$n_1 = \int \mathcal{L}\mathrm{d}t \cdot \left(\frac{\mathrm{d}}{\mathrm{d}\log(-t)} 2\Delta\alpha(t) \right) .$$

The dependence on the integrated luminosity is given explicitly; obviously one has $n_i = u_i \cdot \int \mathcal{L}\mathrm{d}t$ by comparing (8), (9) and (10).

In the ratio n_1/n_0 the dependence of the integrated luminosity drops out:

$$\frac{\mathrm{d}}{\mathrm{d}\log(-t)} \Delta\alpha = \frac{n_1}{2n_0} (1 + 2\Delta\alpha(\langle t \rangle)) .$$

The slope $\mathrm{d}\Delta\alpha/\mathrm{d}\log(-t)$, the quantity of interest, is then directly given by the ratio of the two experimentally measured quantities n_0 and n_1, namely $n_1/2n_0$. The contribution of $2\Delta\alpha(\langle t \rangle)$ is small compared to 1 and can be neglected. The accuracy of the slope is determined by $\delta n_1/2n_0$, i.e. about 10% (see Table 5), which is far smaller than the absolute value of $n_1/2n_0$.

On the other hand, n_0 relates the integrated luminosity to $\Delta\alpha$ at the average value of t, i.e.

$$\int \mathcal{L}\mathrm{d}t = \frac{n_0}{1 + 2\Delta\alpha(\langle t \rangle)} .$$

Making use of $\Delta\alpha(\langle t \rangle)$ as a priori knowledge, the fitted n_0 can be used to derive the integrated luminosity, which is the standard procedure. The statistical precision is given by $\delta n_0/n_0$, which is on the order of 10^{-3}.

In addition, the hadronic contribution to $\Delta\alpha(t)$ (see Fig. 2) may be deduced by subtracting the leptonic contribution, which is theoretically precisely known. The extraction of the hadronic contribution is only limited by the experimental precision.

7 Conclusions

A novel approach to access directly and to measure the running of α in the spacelike region is proposed. It consists in analyzing small angle Bhabha scattering. Depending on the particular angular detector coverage and on the energy of the beams, it allows one to cover a sizeable range of the t-variable.

The feasibility of the method has been put in evidence by the use of a new tool SAMBHA to calculate the small

angle Bhabha differential cross section with a theoretical accuracy to better than 0.1%.

The information obtained in the t-channel can be compared with the existing results of the s-channel measurements. This represents a complementary approach which is direct, transparent and based only on QED interactions and furthermore free of some of the drawbacks inherent in the s-channel methods.

The method outlined can be readily applied to the experiments at LEP and SLC. It can also be exploited by future e^+e^--colliders as well as by existing lower energy machines.

An exceedingly precise measurement of the QED running coupling $\Delta\alpha(t)$ for small values of t may be possibly envisaged with a dedicated luminometer even at low machine energies.

References

1. D.E. Groom et al., Eur. Phys. J. C **15**, 1 (2000)
2. S. Eidelman, F. Jegerlehner, Z. Phys. C **67**, 602 (1995)
3. K. Hagiwara, D. Haidt, S. Matsumoto, C.S. Kim, Z. Phys. C **64**, 559 (1994); Z. Phys. C **68**, 353 (1995); K. Hagiwara, D. Haidt, S. Matsumoto, Eur. Phys. J. C **2**, 95 (1998)
4. F. Jegerlehner, hep-ph/0308117
5. M. Davier, A. Höcker, Phys. Lett. B **435**, 427 (1998); M. Davier, S. Eidelman, A. Höcker, Z. Zhang, Eur. Phys. J. C **27**, 497 (2003)
6. D. Karlen, H. Burkhardt, Eur. Phys. J. C **22**, 39 (2001); hep-ex/0105065
7. A.A. Pankov, N. Paver, Eur. Phys. J. C **29**, 313 (2003)
8. TOPAZ Collaboration, I. Levine et al., Phys. Rev. Lett. **78**, 424 (1997)
9. L3 Collaboration, M. Acciarri et al., Phys. Lett. B **476**, 48 (2000)
10. A.B. Arbuzov, V.S. Fadin, E.A. Kuraev, L.N. Lipatov, N.P. Merenkov, L. Trentadue, Nucl. Phys. B **485**, 457 (1997)
11. S.J. Brodsky, G.P. Lepage, P.B. Mackenzie, Phys. Rev. D **28**, 228 (1983)
12. LEP Working Group, Yellow Report CERN 96-01, Event Generators for Bhabha scattering, Convenors, S. Jadach, O. Nicrosini, p. 229
13. Yellow Report CERN 96-01, description of NLLBHA
14. R. Budny, Phys. Lett. B **55**, 227 (1975)
15. D. Bardin, W. Hollik, T. Riemann, Z. Phys. C **49**, 485 (1991)
16. M. Böhm, A. Denner, W. Hollik, Nucl. Phys. B **304**, 687 (1988)
17. G. Källén, A. Sabry, K. Dan. Vidensk. Selsk. Mat.-Fis. Medd. **29**, (1955) No. 17
18. M. Steinhauser, Phys. Lett. B **429**, 158 (1998); hep-ph/9803313
19. S. Eidelman, F. Jegerlehner, Z. Phys. C **67**, 585 (1995); hep-ph/9502298
20. S. Jadach et al., Event Generators for Bhabha Scattering, CERN Yellow Report 96–01, vol. 2, 1996, p. 229; hep-ph/9602393
21. A. Arbuzov et al., Phys. Lett. B **383**, 238 (1996); hep-ph/9605239
22. A.B. Arbuzov, hep-ph/9907298
23. A.B. Arbuzov, hep-ph/9910280
24. M. Kobel et al. [Two Fermion Working Group Collaboration], Two-fermion production in e^+e^- collisions, hep-ph/0007180, CERN Yellow Report 2000-09-D, p. 115
25. D.Y. Bardin, M.S. Bilenkii, T. Riemann, M. Sachwitz, H. Vogt, Comput. Phys. Commun. **59**, 303 (1990)
26. E.A. Kuraev, V.S. Fadin, Sov. J. Nucl. Phys. **41**, 466 (1985)
27. O. Nicrosini, L. Trentadue, Phys. Lett. B **196**, 551 (1987); Z. Phys. C **39**, 479 (1988)
28. M. Skrzypek, Acta Phys. Polon. B **23**, 135 (1992)
29. A.B. Arbuzov, Phys. Lett. B **470**, 252 (1999); hep-ph/9908361
30. S. Jadach et al., Comp. Phys.Comm. **102**, 229 (1997)
31. P. Abreu et al., Nucl. Instr. Meth. A **378**, 57 (1996)